Hindawi
Advances in Materials Science and Engineering
Volume 2019, Article ID 5465687, 8 pages
https://doi.org/10.1155/2019/5465687

Research Article

Performance Damage Characteristics of Asphalt Binder Suffered from the Action of Sulfate

Rui Xiong,[1,2] **Ning Qiao**,[1] **Fa Yang**,[3] **Ci Chu**,[1] **Liding Li**,[4] **Jiayu Wu**,[1] **Wenyu Jiang**,[1] **Kehong Li**,[1] **and Huaxin Chen**[1,2]

[1]*School of Materials Science and Engineering, Chang'an University, Xi'an 710061, China*
[2]*Engineering Research Center of Transportation Materials of Ministry of Education, Chang'an University, Xi'an 710061, China*
[3]*Yunnan Communications Investment & Construction Group Co., Ltd., Kunming 650228, China*
[4]*School of Transportation, Jilin University, Changchun 130022, China*

Correspondence should be addressed to Rui Xiong; xiongr61@126.com

Received 9 October 2018; Revised 18 January 2019; Accepted 19 March 2019; Published 1 April 2019

Academic Editor: Wei Zhou

Sulfate erosion is a threat to durability and sustainability of pavement structure. In this work, the performance degradation of asphalt binder under internal sulfate erosion was investigated. Different dosages of Na_2SO_4 (0 wt.%, 2.5 wt.%, 5 wt.%, and 10 wt.%) samples were prepared to investigate the effect of sulfate on the performance of the asphalt binder. The surface tension test and low-temperature rheological property test were carried out to evaluate the adhesion of sulfate-incorporated asphalt mastic. Rapid freezing and thawing test with different concentrations of sulfate solution was conducted to explore the effect of sulfate concentrations and freeze-thaw cycles on the softening point and force ductility of matrix asphalt. Phases of the asphalt binder were characterized by Fourier transform infrared (FTIR) spectroscopy. The results show that sulfate has a negative impact on the road performance of the asphalt binder. Internal sulfate erosion decreased the adhesion of the asphalt binder. Also, the low-temperature rheological property of asphalt binder was deteriorated. After the freeze-thaw cycles of external sulfate erosion, softening point and tensile force peak of matrix asphalt increased and the low-temperature ductility decreased. The main reason of performance deterioration of the asphalt binder is the "salt aging" effect causing by sulfate erosion. The research results can provide useful reference for the durability design of asphalt mixture in sulfate-enriched regions.

1. Introduction

Asphalt pavements are the main paving type of highway because of its advantages such as low noise, good skid resistance, improved comfort, convenience of maintenance, and recyclability. However, asphalt pavements are subjected to different levels of durability problems such as high-temperature rutting, low-temperature cracking, moisture damage, and fatigue under the effects of climatic conditions and repeated vehicle loading [1]. Actually, it should be noted that the real service environment for the asphalt pavement is more complex especially in the salt lakes and saline soil regions in western China and other similar regions, where the climate environment is relatively severe [2, 3]. Nowadays, the durability of the asphalt mixture has always been one of the important areas of concern. The erosive media, such as sulfate, enriched in the natural environment often makes road engineering materials suffer from damage to different extent, and freeze-thaw cycles further deteriorate the road performance of asphalt mixture. As a result, asphalt mixture shows severe durability problems [3]. At present, some studies have shown that chlorine salts have a continuing negative effect on asphalt mixture [4–9]. In addition, the adhesion of asphalt under salt action is also a hot research trend. Nowadays, the surface energy theory has been widely used to evaluate the adhesion properties of asphalt and aggregate [10, 11]. However, up to now, little research has been done on the durability of the asphalt binder exposed to sulfate erosion and freeze-thaw circles.

2. Materials and Methods

2.1. Asphalt. The SK-90# matrix asphalt was used for all experiments. Its physical properties were measured following the Standard Test Methods of Bituminous Mixtures for Highway Engineering of China (JTG E20-2011), presented in Table 1.

2.2. Filler. Limestone mineral filler (LMF) and sodium sulfate (Na_2SO_4) powder were used in the test, whose technical indicators are shown in Tables 2 and 3, respectively.

Based on the plug-in method, the contact angles between the surface of asphalt binder and distilled water, glycerin, and glycol liquid were measured. The surface free energy parameters of the three liquids are shown in Table 4.

2.3. Preparation of Sulfate-Incorporated Asphalt Mastic. For practical asphalt pavement engineering projects in China, AC-13 is the most widely used surface paving material. The 0.075 mm sieve passing percentage of mineral aggregate gradations is usually around 5%, and the optimum asphalt content (OAC) is around 5% by the mass of mineral aggregate [12]. So, the filler-binder ratio of the asphalt mastic is 1 : 1. According to current technical specification requirements of China, oven-dried LMF and Na_2SO_4 powder were passed through 0.075 mm sieve, respectively. Fillers passing the 0.075 mm sieve were got to prepared asphalt mastic samples at a mass ratio of 1 : 1 (both of them have similar apparent density). Take the Na_2SO_4 powder asphalt mastic as example, the samples were prepared according to the following procedure. Firstly, asphalt was heated to the desired temperature (145 ± 5°C) in a three-neck flask provided with a stirrer and contact thermometer. Secondly, the temperature was held constant by an automatic control system while stirring lasting for 10 min after Na_2SO_4 powder was dispersed into the asphalt with different percentages. Then, a series of samples could be prepared. The same as the LMF asphalt mastic. The test was carried out by using the matrix asphalt and the sulfate-incorporated asphalt mastic with the age of 30 d and 120 d under the constant temperature conditions for comparison.

2.4. Asphalt Adhesion Based on Surface Energy Theory. Studies have shown that the surface energy (γ) of a substance is mainly composed of a polar component (γ^p) and a nonpolar dispersion component (γ^d). The polar component includes a polar acid component (γ^+) and a polar base component (γ^-). The formula can be represented as follows:

$$\gamma = \gamma^p + \gamma^d = \gamma^d + 2\sqrt{\gamma^+}\sqrt{\gamma^-}. \quad (1)$$

Meanwhile, the Young–Dupre formula for asphalt and the aggregate system can be represented as follows:

$$W_{as} = \gamma_a(1 + \cos\theta) = 2\sqrt{\gamma_a^d}\sqrt{\gamma_s^d} + 2\sqrt{\gamma_a^+}\sqrt{\gamma_s^-} + 2\sqrt{\gamma_s^+}\sqrt{\gamma_a^-}, \quad (2)$$

where θ is the contact angle between asphalt and aggregate, γ_a is the surface energy of the asphalt, γ_s is the surface energy of the aggregate, and γ_a^d and γ_s^d are the nonpolar dispersion components of the asphalt and the aggregate, respectively [13]. Figure 1 shows the surface tension meter and sample to be tested. By measuring the contact angle between asphalt and the aforementioned three liquids with known surface energy parameters, the free energy component and surface free energy of asphalt can be determined according to above equations.

2.5. Rheological Properties of Asphalt Binder Based on Viscoelastic Theory. The bending beam rheological (BBR) test can directly reflect the influence of ambient temperature and time on the low-temperature performance of asphalt materials. Asphalt is a typical viscoelastic material, and the most widely used viscoelastic model is the Burgers model which is a four-component viscoelasticity consisting of a set of Maxwell models and Kelvin models. The Burgers model can effectively describe the viscoelasticity of matrix asphalt, modified asphalt, aged asphalt, and recycled asphalt. The creep compliance formula of the Burgers model can be represented as

$$J_{(t)} = \frac{\varepsilon_{(t)}}{\sigma_0} = \frac{1}{E_1} + \frac{t}{\eta_1} + \frac{1}{E_2}\left(1 - e^{-(E_2 t/\eta_2)}\right) = J_E + J_C + J_V, \quad (3)$$

where J_E is the instantaneous elastic compliance, J_C is the delayed elastic compliance, and J_V is the viscous creep compliance [14].

2.6. Freeze-Thaw Cycle Test Exposed to Na_2SO_4 Solution. The freeze-thaw cycle test exposed to Na_2SO_4 solution in this study mainly focuses on the effect of sulfate concentration and freeze-thaw cycles on the performance change of the asphalt binder. First, the asphalt sample is placed in a square pan, and a sufficient amount of sulfate solution is poured on its surface. Adopting the rapid freeze-thaw test method of cement concrete, the freezing temperature of asphalt is set as −18°C lasting for 2 h and then the melting temperature is as 5°C lasting for 2 h, which is a whole procedure (one time). The concentration of Na_2SO_4 solution is selected as 0% (distilled water), 2.5%, 5%, and 10%. The number of freeze-thaw cycles is set as 7 times, 14 times, 21 times, and 28 times. The performance of asphalt exposed to Na_2SO_4 solution was evaluated through the softening point and force ductility test. The freeze-thaw cycle test exposed to Na_2SO_4 solution is shown in Figure 2.

3. Results and Discussion

3.1. Sulfate-Incorporated Asphalt Mastic

3.1.1. Contact Angle Test. The results of the contact angle for the matrix asphalt and sulfate-incorporated asphalt mastic versus above three liquids (distilled water, glycerin, and ethylene glycol) are shown in Table 5, which satisfies the

Table 1: Technical properties of SK-90# asphalt binder.

Test items		Unit	Technical requirements	Value	Specification
Penetration	15°C, 100 g, 5 s	0.1 mm	Non	43	T0604
	25°C, 100 g, 5 s		80~100	86	
	30°C, 100 g, 5 s		Non	160	
Softening point (R&B)		°C	≥44	47.0	T0606
Ductility (15°C, 5 cm/min)		Cm	≥100	≥100	T0605
Flash point		°C	≥260	304	T0611
Solubility		%	≥99.5	99.8	T0607
Specific gravity (15°C)		g/cm^3	Non	1.030	T0603
RTFOT (163°C, 75 min)	Mass loss	%	±0.8	0.15	T0610
	Penetration ratio (25°C)	%	≥57	60.5	T0604
	Ductility (10°C)	cm	≥8	9.8	T0605

Table 2: Technical properties of LMF.

Test items	Unit	Technical requirements	Value	Specification
Apparent density	g/cm^3	≥2.50	2.705	T0352
Water content	%	≤1	0.429	T0103
Gradation				
<0.6 mm	%	100	100	T0351
<0.15 mm	%	90–100	97.8	T0351
<0.075 mm	%	75–100	95.1	T0351
Hydrophilic coefficient	—	<1	0.31	T0353

Table 3: Technical indicators of sodium sulfate.

Ingredient	Na_2SO_4	Cl	Ca, Mg	Fe	Water insoluble	Apparent density (g/cm^3)	Solubility (g) (20°C)
Content (%)	≥99	≤0.35	≤0.15	≤0.002	≤0.05	2.690	19.5

Table 4: Surface free energy parameters of three fluids (mJ/m^2).

Liquid type	γ_L	γ_L^d	γ_L^p	γ_L^+	γ_L^-
Distilled water	72.8	21.8	51.0	25.5	25.5
Glycerin	63.4	37.0	26.4	3.92	57.4
Ethylene glycol	48.3	29.3	19.0	1.92	47.0

accuracy requirement. In the case of sulfate-incorporated asphalt mastic, the contact angle between asphalt and different liquids increases to some extent along with the increase of age. That is, the "salt aging" effect increases the hydrophilicity of the asphalt mastic. At the same tested liquid condition, the contact angles between the sulfate-incorporated asphalt mastic and the liquids are greater than that of matrix asphalt and the liquids. Based on the wetting theory, in the presence of sulfate, the wettability of the asphalt to the aggregate is reduced to some extent, and further weakens with the increase of age, which directly leads to the decrease of the adhesion between asphalt and aggregate, thereby affecting the road performance of asphalt mixture.

The contact angle values in Table 5 are brought into the above formulas to obtain the dispersion component (γ_s^d), the polar acid component (γ_s^+), and the polar base component (γ_s^-) of various asphalt mastics. Then, the surface free energy can be calculated. The results of surface free energy and its components of matrix asphalt and asphalt mastics are shown in Figure 3.

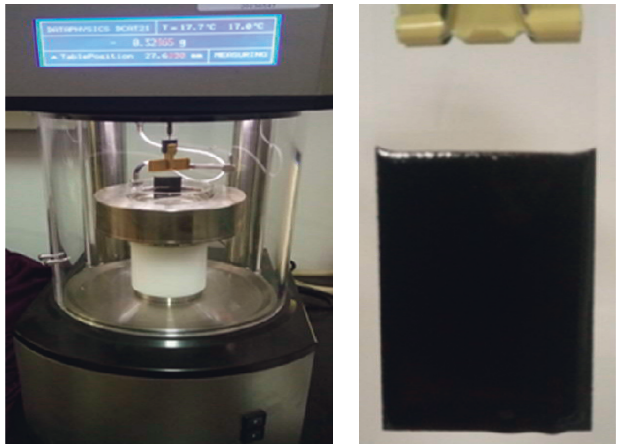

(a) (b)

Figure 1: Surface tension meter and sample to be tested.

It can be seen from Figure 3, compared with the matrix asphalt, the surface free energy and polar components of the LMF asphalt mastic are improved while the nonpolar component is significantly reduced at 30 d and 120 d ages, indicating that the incorporation of LMF enhances the polarity of the asphalt and improves the surface tension. Compared with the LMF asphalt mastic, the surface free energy of Na_2SO_4 asphalt mastic decreased significantly at 30 d and 120 d ages. The surface free energy of the Na_2SO_4

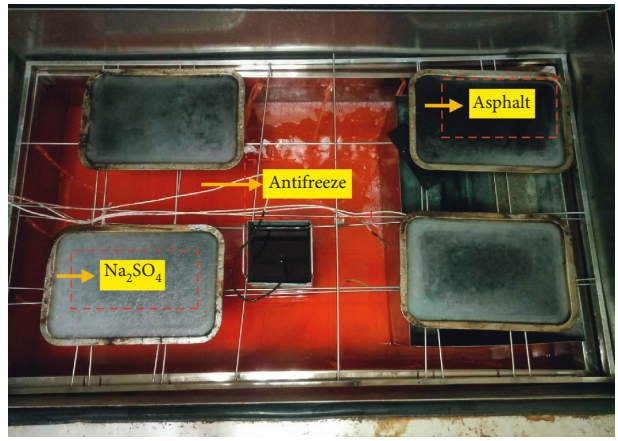

Figure 2: Freeze-thaw cycle test in the environmental cabinet.

Table 5: Contact angle between asphalt mastic and liquids.

Asphalt	Distilled water		Glycerin		Ethylene glycol	
	Average (°)	Coefficient of variation (%)	Average (°)	Coefficient of variation (%)	Average (°)	Coefficient of variation (%)
Matrix	112.85	1.46	103.84	0.29	81.97	1.46
LMF 30	117.64	1.22	105.72	0.35	82.58	1.41
LMF 120	119.37	1.53	106.99	0.36	90.97	0.94
Na_2SO_4 30	117.54	1.75	108.38	0.71	82.35	1.51
Na_2SO_4 120	118.10	0.58	109.16	0.98	86.70	0.99

asphalt mastic shows a downward trend. According to the calculated cohesive and adhesion power, sulfate incorporation reduces the free energy and dispersion component of the asphalt surface, which in turn adversely affects the water sensitivity of asphalt mixture.

3.1.2. BBR Test. The test results of stiffness modulus S and creep rate m of various asphalt mastics at the temperature of −6°C, −12°C, −18°C, and −24°C are shown in Figure 4.

It can be seen from Figure 4 that, at the same temperature, compared with the matrix asphalt, the stiffness modulus of the sulfate-incorporated asphalt mastic increases greatly, and the creep rate decreases, indicating that the sulfate deteriorates the low-temperature performance of the asphalt binder. As the age increases, performance of the sulfate-incorporated asphalt mastic continues to deteriorate. In addition, the incorporation of sulfate hardens the asphalt to a certain extent, forming the "salt aging" effect as mentioned before. Meanwhile, under low-temperature conditions, the asphalt is in a glassy state, and the asphalt molecular chain is difficult to be rapidly oriented or moved.

Then, the results of the BBR test were fitted by Origin 8.5 software. The elastic moduli E_1 and E_2, viscosity coefficients η_1 and η_2, the relaxation time λ, and delay time τ of the Burgers model were obtained at different temperatures, shown in Table 6.

It can be seen from Table 6, the variation of delay time λ of the asphalt mastics at different ages in the temperature range of −12°C~−6°C shows that the matrix asphalt has the smallest change, and the Na_2SO_4 asphalt mastic changes the most. At the same temperature, the longer the age, the worse

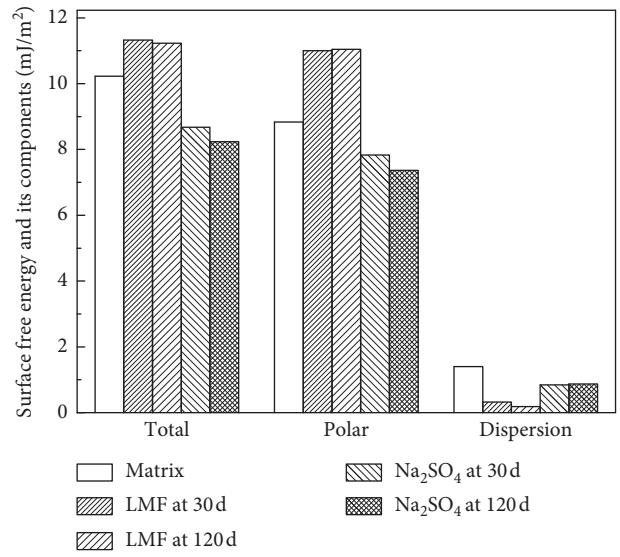

Figure 3: Surface free energy and its components of matrix asphalt and asphalt mastics.

low-temperature performance of the sulfate-incorporated asphalt mastics. As the temperature decreases, the relaxation time of various asphalt mastics is gradually prolonged. On the one hand, the movement of the asphalt molecular chain is subject to increasing internal frictional resistance, and the stress relaxation is slowed down. On the other hand, the temperature reduction reduces the energy consumption rate and increases the relaxation time. Within the entire test temperature range, the stress relaxation ability

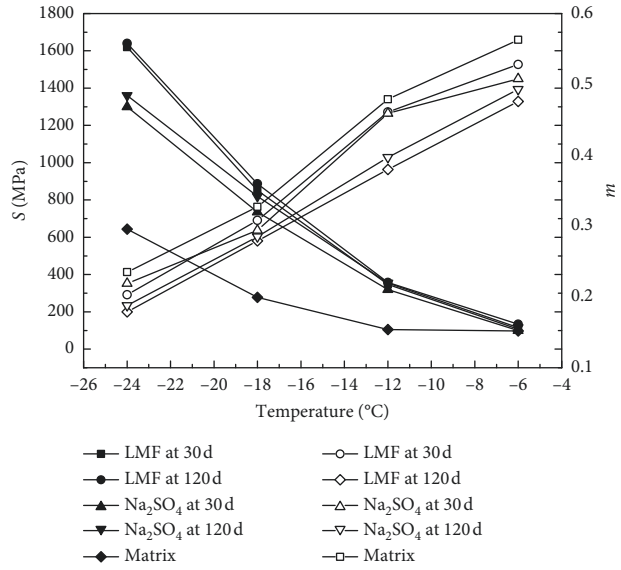

Figure 4: Stiffness modulus S and creep rate m of asphalt mastic at different temperatures.

Table 6: Results of Burgers' parameters of asphalt mastics at different temperatures.

Temperature (age)	Asphalt	E_1 (MPa)	η_1 (MPa·s)	E_2 (MPa)	η_2 (MPa·s)	λ (s)	τ (s)
−6°C (30 d)	Matrix	346.79	4932.53	196.72	937.23	14.2	4.8
	LMF	782.53	12554.31	290.73	2474.54	16.0	8.5
	Na_2SO_4	730.59	12834.00	275.46	2418.66	17.6	8.8
−6°C (120 d)	LMF	912.99	17624.22	342.42	3097.03	19.3	9.0
	Na_2SO_4	768.39	15581.16	318.66	2793.52	20.3	8.8
−12°C (30 d)	Matrix	527.98	16707.08	262.37	2729.59	31.6	10.4
	LMF	1550.60	49238.56	1037.81	8772.50	31.8	8.5
	Na_2SO_4	1266.20	63975.90	741.95	9754.37	50.5	13.1
−12°C (120 d)	LMF	1560.36	72375.70	835.49	9732.53	46.4	11.6
	Na_2SO_4	1253.03	48445.35	775.89	8272.98	38.7	10.7
−18°C (30 d)	Matrix	798.17	68529.06	688.81	9428.90	85.9	13.7
	LMF	2091.98	234840.90	2209.36	34816.08	112.3	15.8
	Na_2SO_4	1767.52	206386.83	1954.40	29102.74	116.8	14.9

of the sulfate-incorporated asphalt mastic is inferior to the LMF asphalt mastic.

3.2. Freeze-Thaw Cycle Test Exposed to Na_2SO_4 Solution

3.2.1. Softening Point. The softening point of the matrix asphalt sample with 7, 14, 21, and 28 times of freeze-thaw cycles was tested, respectively, exposed to 0%, 2.5%, 5%, and 10% Na_2SO_4 solution. The results are shown in Figure 5.

It can be seen from Figure 5 that, for the same concentration of sulfate solution, as the freeze-thaw cycles increases, the softening point of the matrix asphalt increases with different degrees. Under the same freeze-thaw cycles, the higher the concentration of the sulfate solution, the greater the softening point of the asphalt. When the concentration of sulfate solution is small, the increase of freeze-thaw cycles has little effect on the softening point value. When the concentration reaches 10%, the change of freeze-

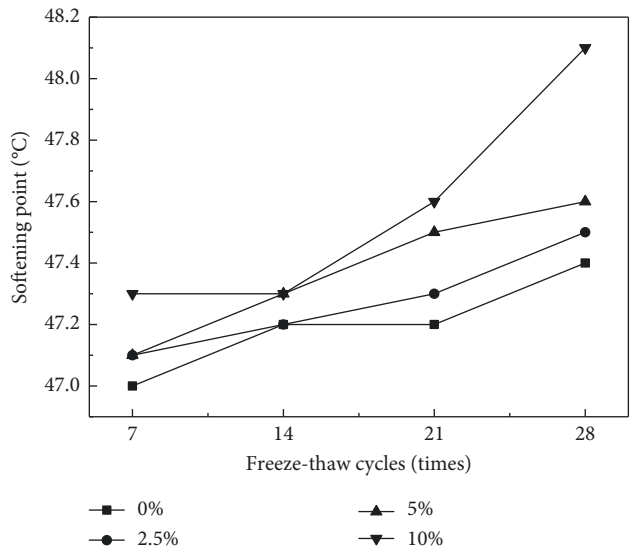

Figure 5: Softening point of asphalt exposed to freeze-thaw cycles.

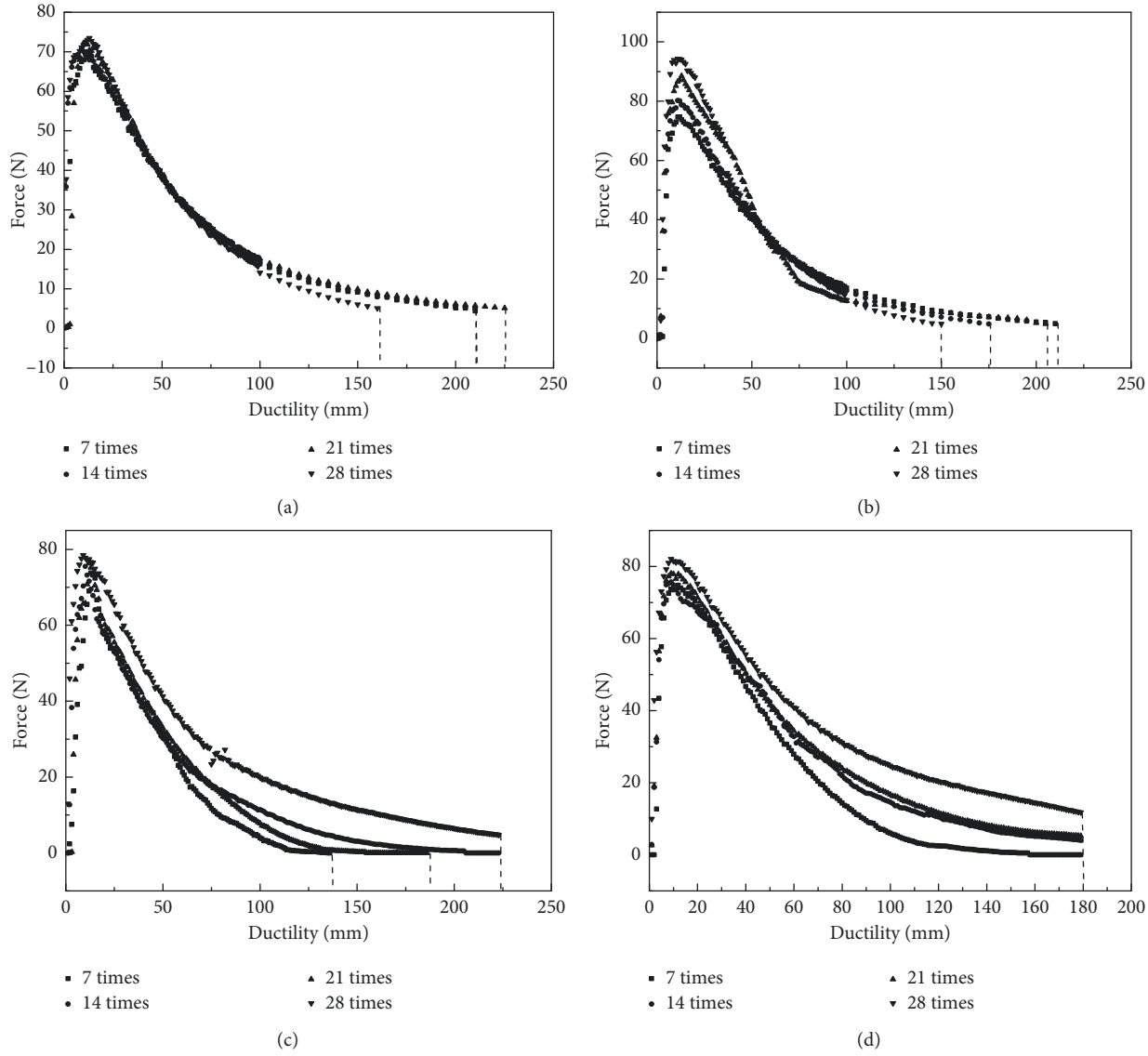

Figure 6: Force ductility test results: (a) 0% Na_2SO_4, (b) 2.5% Na_2SO_4, (c) 5% Na_2SO_4, and (d) 10% Na_2SO_4.

thaw cycles will increase the softening point significantly. Compared with distilled water, the sulfate solution has a certain enhancement effect on the softening point. After different freeze-thaw cycles, the asphalt gradually changes from the sol-type structure to the gel-type structure, and the proportion of asphaltenes becomes higher while the outer film of the micelles becomes thinner. The macroperformance is that the asphalt becomes more harden and brittle.

3.2.2. Force Ductility. The force ductility tester was used to test the change of low-temperature ductility, maximum tensile force of asphalt at 5°C under different sulfate solution concentrations and different freeze-thaw cycles. The results are shown in Figure 6.

It can be seen from Figure 6 that, for the matrix asphalt under the condition of freeze-thaw cycles with distilled water, the increase of freeze-thaw cycles has little effect on the maximum tensile force. When the concentration of sulfate solution is 2.5% and 5%, the maximum tensile force of asphalt goes up with the increase of freeze-thaw cycles. The maximum pull force is quite different. For the 0% and 2.5% sulfate solutions, the fracture ductility of asphalt decreases with the increase of freeze-thaw cycles, and for the 5% and 10% sulfate solutions, the ductility between 7 and 14 times is quite different. In addition, as the freeze-thaw cycles increase, the asphalt elongation changes little. When the tensile force reaches the peak, it quickly enters the stress relaxation phase, and the tensile force decreases rapidly.

The maximum tensile force value of asphalt after freeze-thaw cycles is shown in Figure 7.

It can be seen from Figure 7 that, as the freeze-thaw cycles increases, the peak value of asphalt tensile force increases. When the concentration of the sulfate solution is 2.5%, the peak value of the tensile force is the largest. After

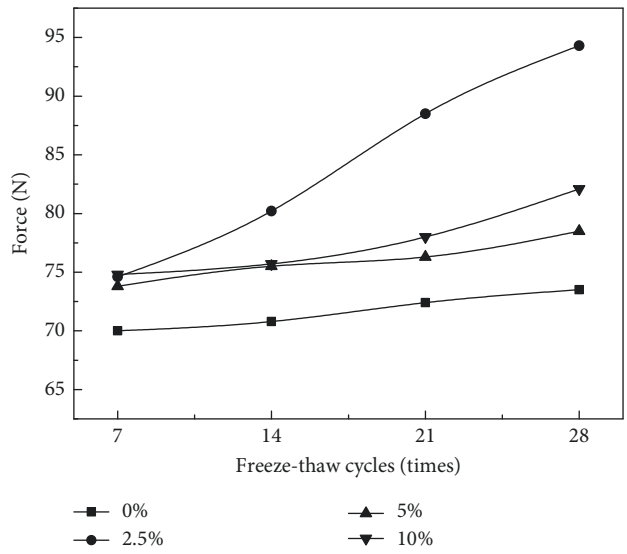

Figure 7: Maximum tensile force of asphalt.

the freeze-thaw cycles, the brine evaporates and the sulfate accumulates on the surface and invades gradually, changing the continuous state of the asphalt.

3.3. Mechanism Analysis of the Action of Sulfate Erosion. Fourier-transform infrared (FTIR) spectroscopy was used to analyze the changes of the absorption peaks of the main functional groups of the matrix asphalt and the above several asphalt mastics (30 d and 120 d). The results are shown in Figure 8.

It can be seen from Figure 8 that the change of the absorption peak of the Na_2SO_4 asphalt mastic at 30 d and 120 d age is that the peak of 1110.63 cm^{-1} is stronger. Compared with the LMF, the Na_2SO_4 has a great influence on the absorption peak of 1605 cm^{-1} for aromatic hydrocarbons and the benzene ring substitution region of 900~650 cm^{-1}, which is the main change of asphalt performance caused by Na_2SO_4. That can be called the aforementioned "salt aging" effect.

4. Conclusions

Due to the prevalence of the sulfate environment in China, this paper aims at exploring the performance damage characteristics of the asphalt binder under the action of sulfate (Na_2SO_4) from internal and external pathways. Some interesting conclusions can be drawn as follows:

(i) For the sulfate-incorporated asphalt mastic, due to the "salt aging" effect, the contact angle of the asphalt binder is obviously increased, and the surface free energy of the sulfate-incorporated asphalt mastic is reduced. Thereby, the adhesion is decreased correspondingly. Meanwhile, the creep rate decreases with the increase of age, and the delay time increases, causing the low-temperature rheological property deteriorate.

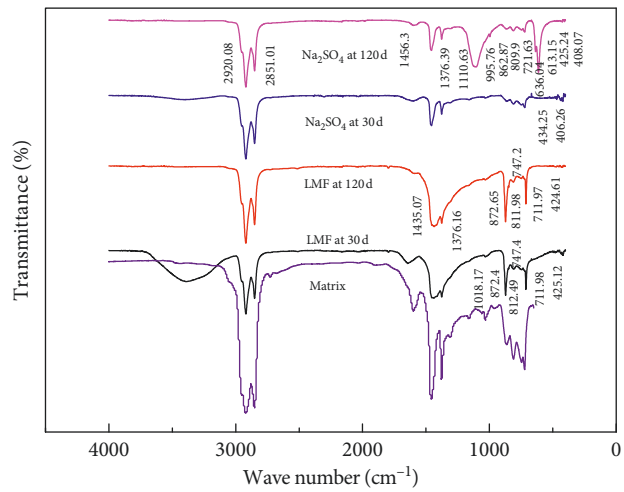

Figure 8: Infrared spectrogram of matrix asphalt and asphalt mastics.

(ii) For the matrix asphalt exposed to the freeze-thaw cycle of Na_2SO_4 solution, as the freeze-thaw cycles increase, the asphalt elongation decreases overall while the maximum tensile force increases gradually. Compared with distilled water (control sample), the presence of Na_2SO_4 makes the low-temperature plasticity of the asphalt get worse.

(iii) Sulfate has a negative impact on the road performance of the asphalt binder. The effect of sulfate on the durability of asphalt and asphalt mixture should be taken into full consideration in sulfate-enriched regions.

Data Availability

The authors would like to declare that all the data in the manuscript were obtained by experiment and the data are true and effective in the manuscript.

Conflicts of Interest

The authors declare that they have no conflicts of interest.

Acknowledgments

The authors wish to thank the financial support from the National Natural Science Foundation of China (no. 51608046), the China Postdoctoral Science Foundation (no. 2014M550476), the Preeminent Youth Fund of Chang'an University (no. 310831163501), and the Fundamental Research Funds for the Central Universities, CHD (no. 300102319202).

References

[1] R. Xiong, L. Wang, B. W. Guan et al., "Durability prediction of asphalt mixture exposed to Sulfate and dry-wet circle erosion environment," *International Journal of Pavement Research and Technology*, vol. 8, no. 1, pp. 53–57, 2015.

[2] B. H. Setiadji, S. Utomo, and N. Nahyo, "Effect of chemical compounds in tidal water on asphalt pavement mixture," *International Journal of Pavement Research and Technology*, vol. 10, no. 2, pp. 122–130, 2017.

[3] J. W. Han, Y. N. Cui, J. D. Li et al., "Microstructure and rheological properties at low-temperature of modified asphalt under salt freezing cycle," *Acta Materiae Compositae Sinica*, vol. 33, no. 8, pp. 1718–1724, 2016.

[4] J. Ahmad, N. I. M. Yusoff, M. R. Hainin, M. Y. A. Rahman, and M. Hossain, "Investigation into hot-mix asphalt moisture-induced damage under tropical climatic conditions," *Construction and Building Materials*, vol. 50, no. 15, pp. 567–576, 2014.

[5] R. Xiong, B. W. Guan, and Y. P. Sheng, "Anti-fatigue property of brucite fiber reinforced asphalt mixture under sulfate and dry-wet circle corrosion environment," *Journal of Wuhan University of Technology*, vol. 36, no. 10, pp. 45–51, 2014.

[6] X. Y. Huang, A. M. Sha, and W. Jiang, "Effect and mechanism of salt erosion on performance of bitumen and asphalt mixtures," *Journal of Chang'an University (Natural Science Edition)*, vol. 37, no. 3, pp. 33–38, 2017.

[7] R. Pittenger and T. R. West, *Effects of Salt and Trace Minerals for Bituminous Pavements Literature Review, Information Gathering and Research Plan Development*, Purdue University, West Lafayette, IN, USA, 1995.

[8] Y. Hassan, A. O. Halim, A. G. Razaqpur et al., "Effects of new deicing alternatives on airfield asphalt concrete pavement," in *Proceedings of the Federal Aviation Administration Technology Transfer Conference*, Atlantic City, NJ, USA, May 2002.

[9] B. Amini and S. S. Tehrani, "Simultaneous effects of salted water and water flow on asphalt concrete pavement deterioration under freeze–thaw cycles," *International Journal of Pavement Engineering*, vol. 15, no. 5, pp. 383–391, 2014.

[10] K. Zhang, R. Luo, and D. R. Zhang, "Wettability analysis on colored resin asphalt binder based on surface free energy theory," *China Journal of Highway and Transport*, vol. 29, no. 5, pp. 34–40, 2016.

[11] T. Valentová, J. Altman, and J. Valentin, "Impact of asphalt ageing on the activity of adhesion promoters and the moisture susceptibility," *Transportation Research Procedia*, vol. 14, pp. 768–777, 2016.

[12] S. Wu, J. Zhu, J. Zhong, and D. Wang, "Experimental investigation on related properties of asphalt mastic containing recycled red brick powder," *Construction and Building Materials*, vol. 25, no. 6, pp. 2883–2887, 2011.

[13] L. Li, Q. Wang, H. Li, B. Li, and Y. Wang, "Adhesion of aged SBS modified asphalt binder containing warm mix additive based on surface free energy," *Cailiao Daobao/Materials Review*, vol. 31, no. 8, pp. 129–149, 2017.

[14] G. Polacco, J. Stastna, and L. Zanzotto, "Accumulated strain in polymer-modified asphalts," *Rheologica Acta*, vol. 47, no. 5-6, pp. 491–498, 2008.